Equipotential Surfaces of a Plasma Moving in a Toroidal Octupole Magnetic Field

A. B. Filimonov
J. C. Sprott
D. E. Lencioni
R. L. Willig

PLP 72
COPY____

University of Wisconsin
Thermonuclear Plasma Studies

COO-1233-32

Equipotential Surfaces of A Plasma Moving in a Toroidal Octupole Magnetic Field*

A. B. Filimonov, J. C. Sprott,
D. E. Lencioni, R. L. Willig

* Work Supported by U. S. Atomic Energy Commission

COO-1233-32

Equipotential Surfaces of a Plasma Moving in a Toroidal Octupole Magnetic Field*

A. B. Filimonov, J. C. Sprott, D.E. Lencioni, R. L. Willig

University of Wisconsin
Physics Department

(Presented at the June 1966 Minneapolis Meeting of the Division of Plasma Physics of the American Physical Society)

ABSTRACT

Measurements of the floating potential resulting from a 100 eV hydrogen plasma moving in a toroidal octupole magnetic field of a few kilogauss revealed a definite structure and time evolution of the equipotentials. It has been found that in areas of relatively high density ($10^{10} cm^{-3}$) i.e., in the central region of the toroid, the magnetic field lines were equipotential surfaces. These surfaces (and consequently the $\vec{E} \times \vec{B}/B^2$ drift) agreed qualitatively with solutions found by J. W. Poukey[1] for describing the drift in a uniform magnetic field, i.e., plasma separated into two sections which circulated in such a manner that the cloud propagated perpendicular to the magnetic field.

---

1. J. W. Poukey, Bull. Am. Phys. Soc. II, 11, 452 (1966)

* Work Supported by the U. S. Atomic Energy Commission

INTRODUCTION

The experiment to be described in this paper was performed on the Wisconsin toroidal octupole,[2] which is shown schematically in Figure 1. A 100eV hydrogen plasma is produced by a conical pinch gun and drifts freely for about 1 meter through a differential pumping chamber before entering the toroid through collimating slots. The plasma enters the octupole region by developing an electric polarization field, and then splits into two blobs which travel circumferentially around the machine, colliding on the opposite side.

Potentials were measured with electrostatic probes located at various ports around the machine. The probes were of a special attenuated type,[3] with an input resistance of 10 megΩ and capacitance of 1 pf, permitting measurement of floating potential for densities as low as 10^7 cm^{-3} with a frequency response of 10 MHz. Although the probes read floating potential, the electron temperature was sufficiently constant that the plasma potential could be obtained by adding a constant voltage, in our case, about 25 volts. Density measurements were made with a special biased double probe which had an input resistance of 1 meg Ω and capacitance of 1 pf, and a frequency response of 1 MHz.

The data discussed here were taken at port 8 and port 2 located at $\pm 50^\circ$ from the injection port, and at a

---

2. Dory, Kerst, Meade, Wilson, Erickson, Phys. Fluids, 9 997 (1966).

3. J. C. Sprott, to be published July, 1966 in Rev. Sci. Instr.

special port located directly above a rod. The times of interest are between 10 and 20 μsec after the gun discharge. This corresponds to the time between the injection and the collision, during which the bulk motion of the plasma is transverse to the magnetic field.

Figure 2 shows a cross section of the octupole magnetic field which is formed by the current in four copper rods and by the image currents in the walls.

APPLICABILITY OF POUKEY'S MODEL

The behavior of a collisionless plasma moving through a uniform transverse magnetic field has been treated theoretically by Poukey,[4] subject to the conditions that drift velocities are small compared with thermal velocities and gyroradii are small.

With a typical density of 10^{10} cm^{-3} in the toroid, the electron-ion collision time is about 100 μsec. This is sufficiently long compared to times of interest that the plasma can be considered collisionless. The magnetic field is certainly not uniform except perhaps very near the walls and behind the rods. The $\vec{E} \times \vec{B}$ drift velocity and ion thermal velocity are both about 10^7 cm/sec. The ion gyroradius is about 2 cm at the outside wall where the field is 1 kilogauss and about 1 cm at the inside wall where the field is 2 kilogauss. The characteristic distance over which potentials change is about the same as the gyroradius. In spite of the

---

4. Poukey, ibid.

fact that Poukey's assumptions are not well satisfied, the experimental results are in qualitative agreement with his solutions.

EXPERIMENTAL RESULTS

Figure 3 shows typical oscilloscope traces of floating potential and density. The noise during the first 10 μsec is RF pickup from the gun and electronics. Scans were made taking 3 shots at each position of the probe in order to average out the shot to shot variation. The polaroid pictures were measured on a measuring table used by the high energy group to measure bubble chamber pictures. The data were digitized and fed into a computer programmed to plot out curves as a function of probe position.

First, an attempt was made to test the extent to which potentials are constant along magnetic field lines. Figure 4 shows the various probe scans which were made at port 2. Field lines are numbered from $\psi = -5$ at the rods to $\psi = +5$ at the walls. The potentials are plotted as a function of ψ for the various scans at 15 μsec after the gun fires. Within the accuracy of the measurements, these curves show that the potential is approximately constant along ψ lines.

Figure 5 shows the potential at port 8 as a function of ψ for the plasma blob travelling in the opposite direction around the machine. The potentials are reversed

because the direction of motion is reversed, but the shape of the curves is the same.

Figure 6 shows the potential as a function of position across the midplane at 15 μsec and as a function ψ, comparing the inside and outside ψ lines. Also plotted is the $\vec{E} \times \vec{B}$ drift velocity as a function of position, showing the plasma moving forward near the center and backward near the outside.

Figure 7 shows the potential and drift velocity at the rod port. The results here are of particular importance because the experimental conditions agree fairly well with Poukey's assumptions. The scatter in data points gives some idea of the reproducibility of the plasma. At this port, all the ψ lines are crossed in one scan and the double vortex motion is clearly seen in the velocity profile.

Figure 8 shows potential surfaces as a function of time and position across the midplane. If the plasma moves with a constant angular velocity around the toroid without appreciable distortion as measurements at different azimuths suggest, the abscissa of this figure can be thought of as angular position. Once this velocity is known, the potentials can be calculated in the frame moving with the plasma. This transformation pushes the potential peaks in toward the center and makes them less pronounced. The x's in the figure show the approximate location of the circulation centers in the moving frame.

Figure 9 shows the potential surfaces at the rod port. As a function of ψ, the contours are nearly symmetrical. In the frame moving with the plasma, the centers of circulation are considerably displaced toward the center, as indicated by the x's.

Figure 10 shows surfaces of equal density across the midplane. Two peaks are observed, but they are somewhat closer together than are the circulation centers. It is likely that since the plasma cylinders have not had ample time to accomplish a complete rotation, a steady-state has not been reached. The density does not go to zero at the center as might be expected, but this is probably because the magnetic field is zero at the center, and the model is not valid.

At the rod port, the electric fields are large and reliable density measurements have not been made.

FIGURES:

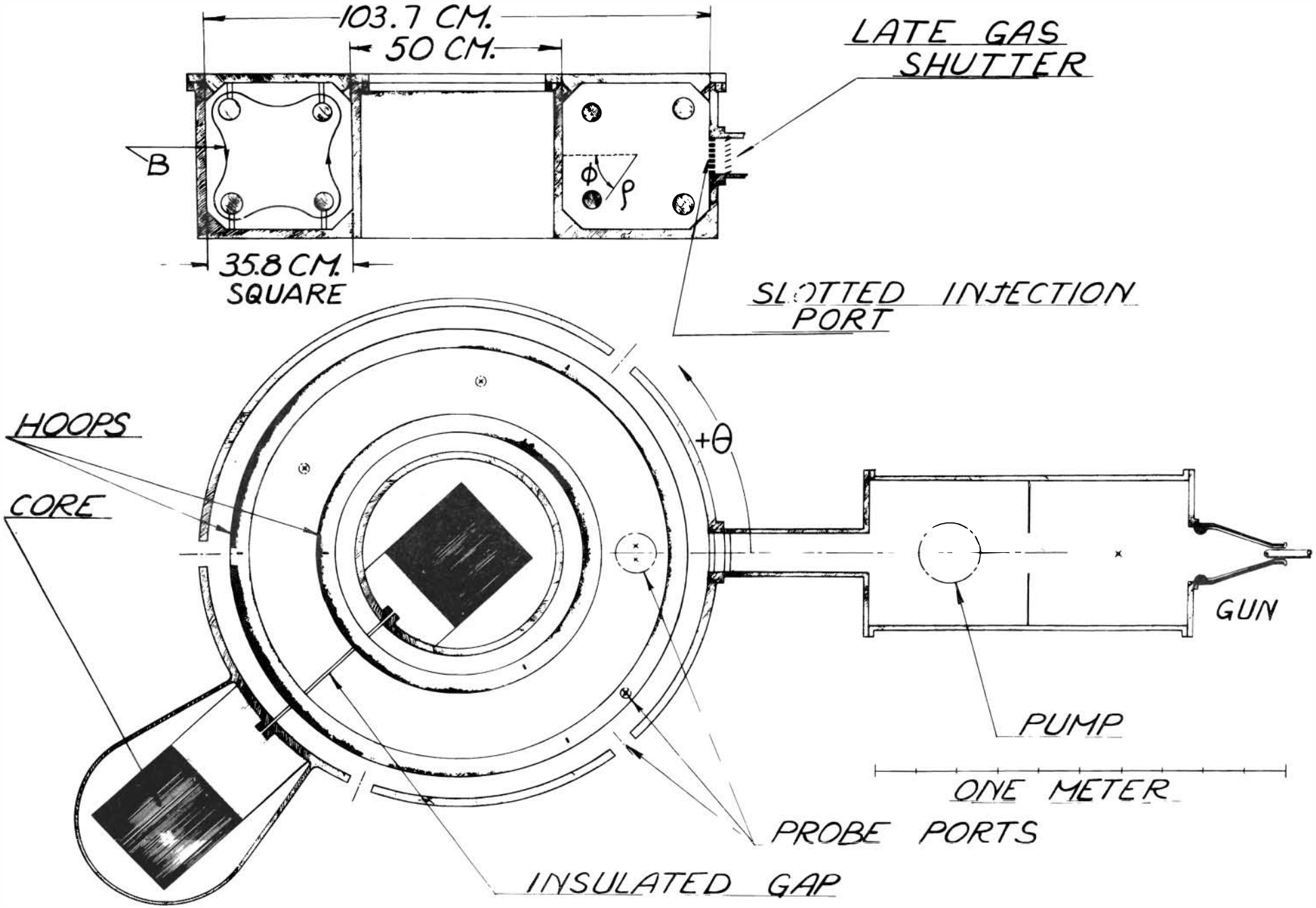
103.7 CM.
50 CM.
LATE GAS SHUTTER
B
35.8 CM. SQUARE
SLOTTED INJECTION PORT
HOOPS
CORE
+θ
GUN
PUMP
ONE METER
PROBE PORTS
INSULATED GAP

Fig 1

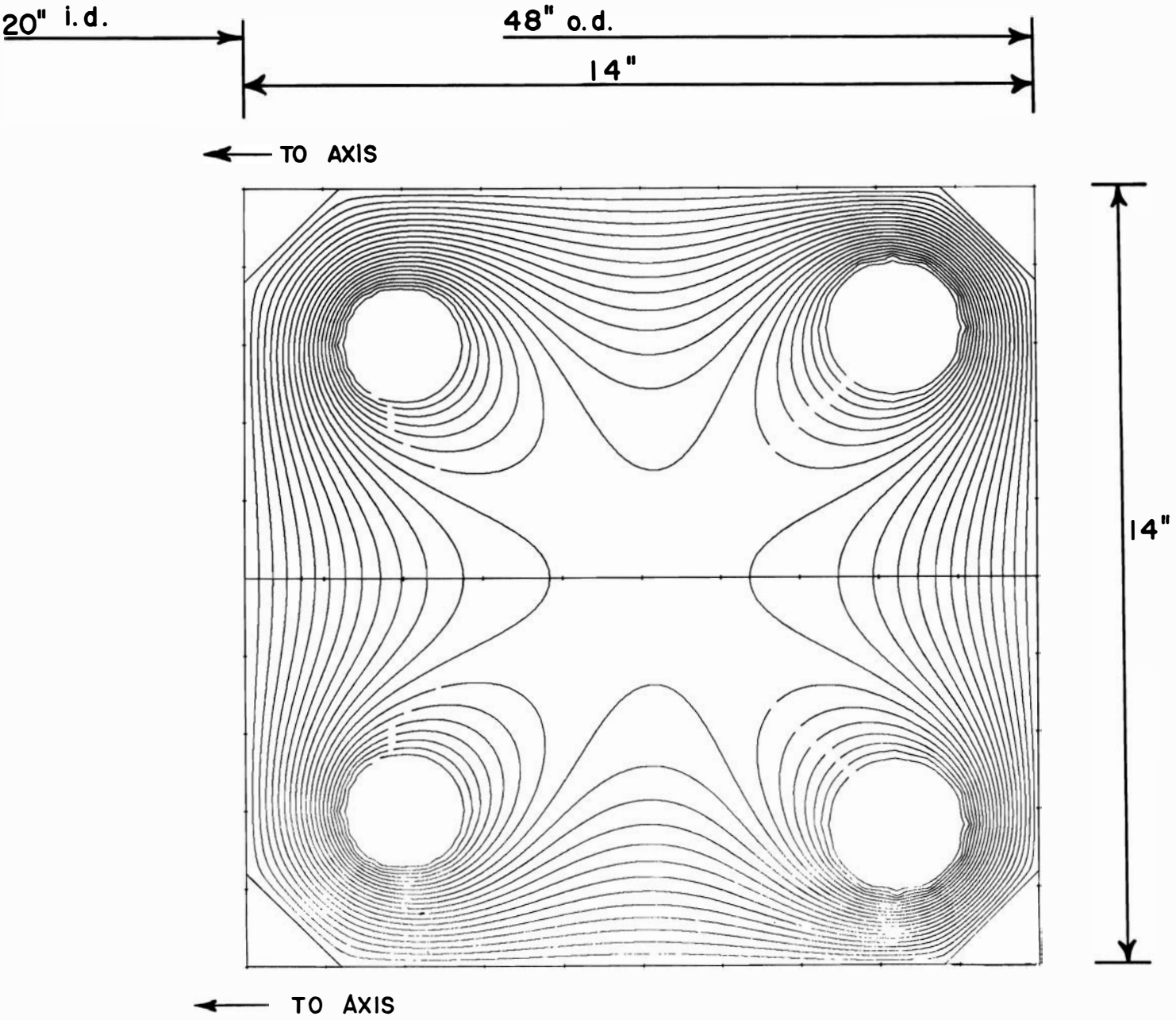

WISCONSIN TOROIDAL OCTUPOLE

Fig. 2

TYPICAL OSCILLOSCOPE TRACES

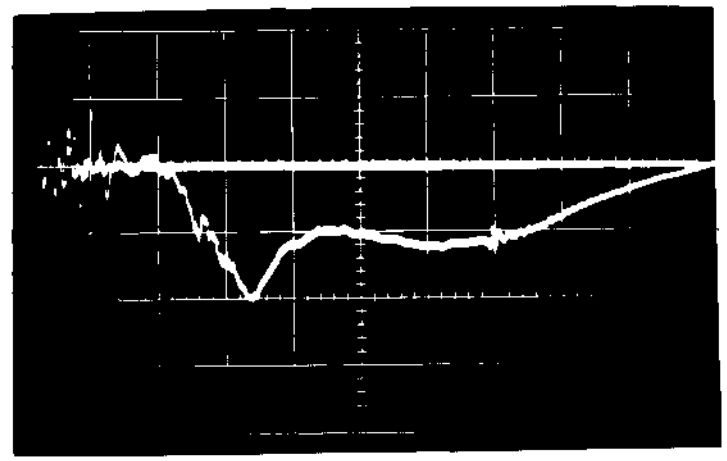

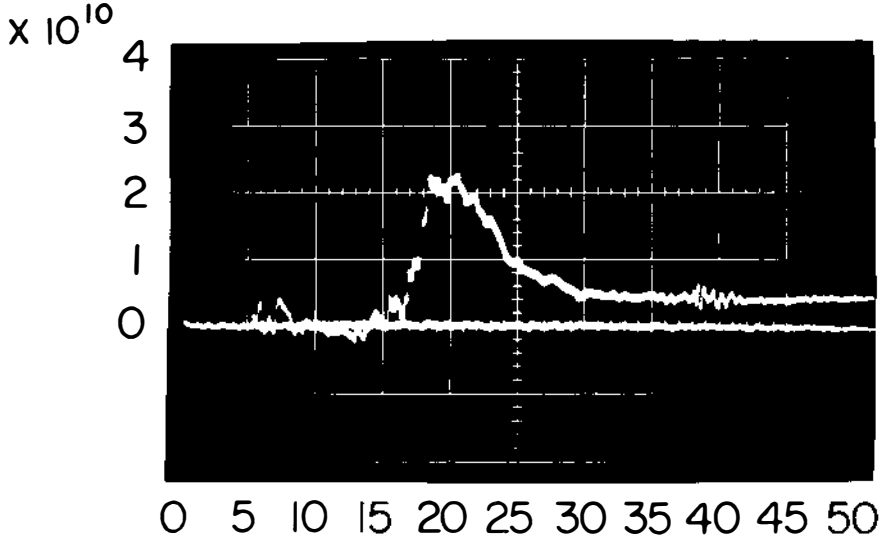

Fig. 3

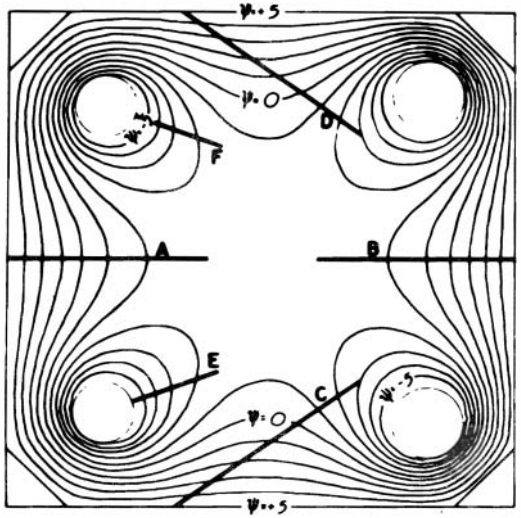

OCTUPOLE FIELD PATTERN

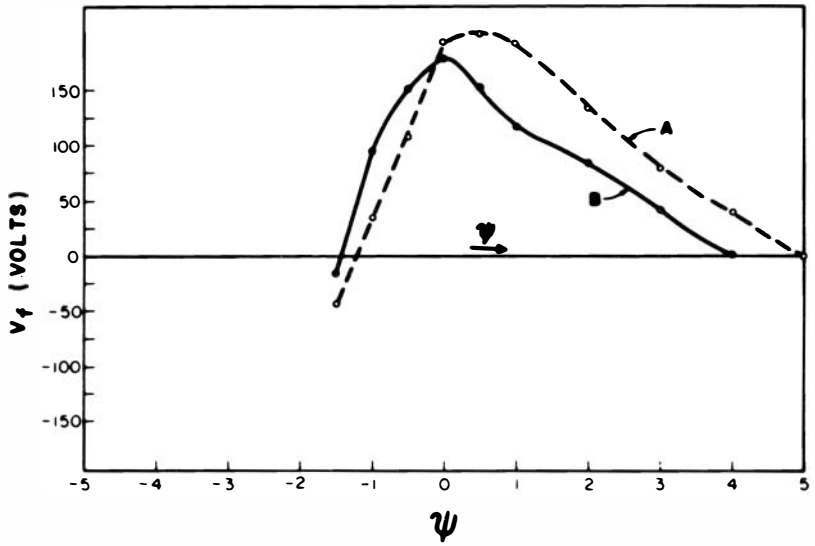

(b)

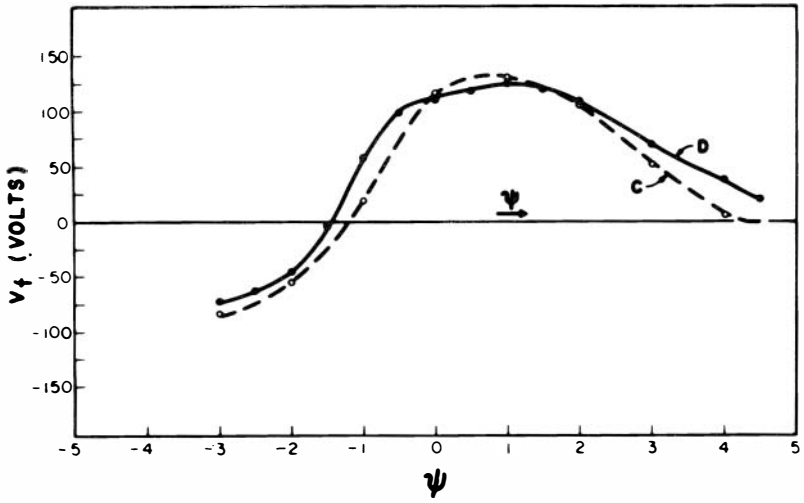

(c)

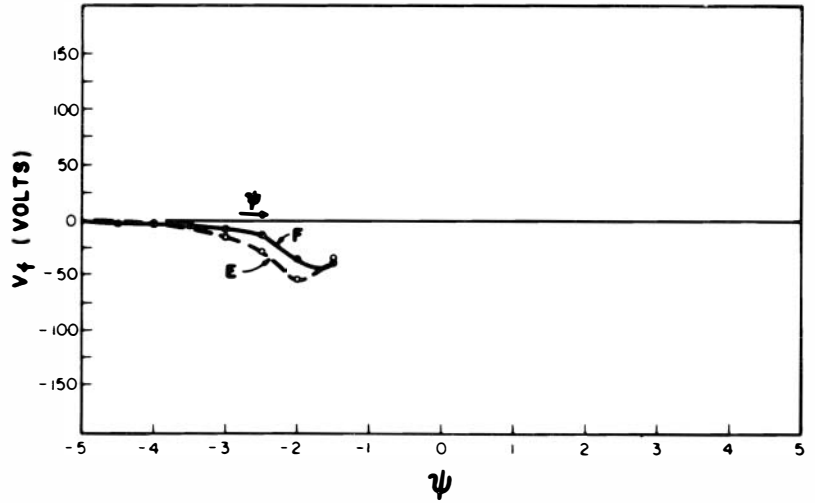

(d)

POTENTIALS AT 15μSEC. VS. ψ FOR VARIOUS SCANS AT P-2

Fig 4

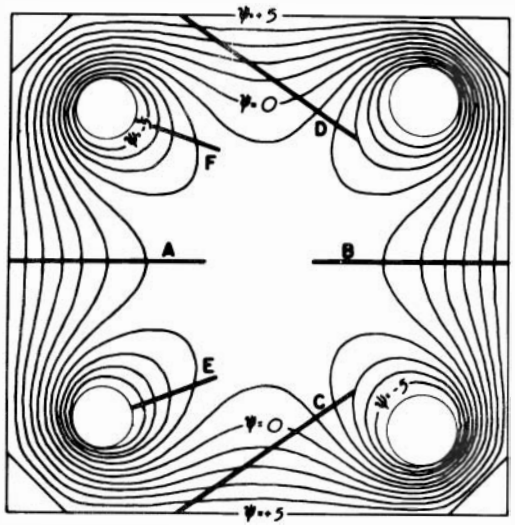

OCTUPOLE FIELD PATTERN

(a)

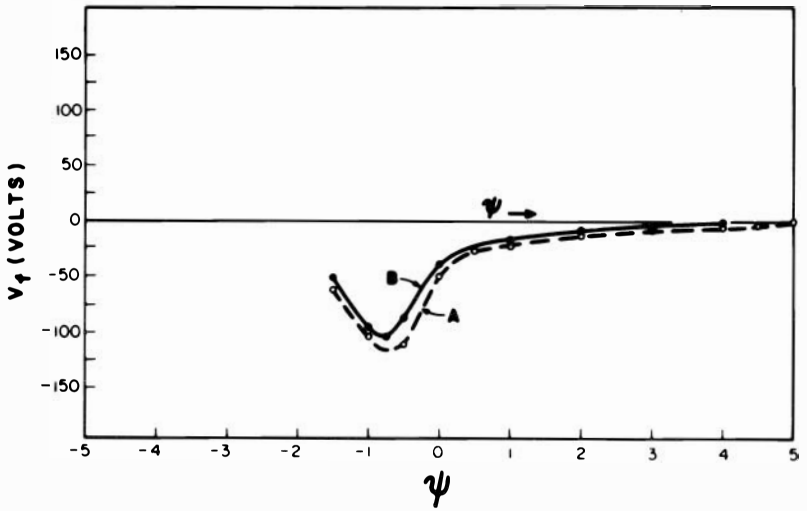

(b)

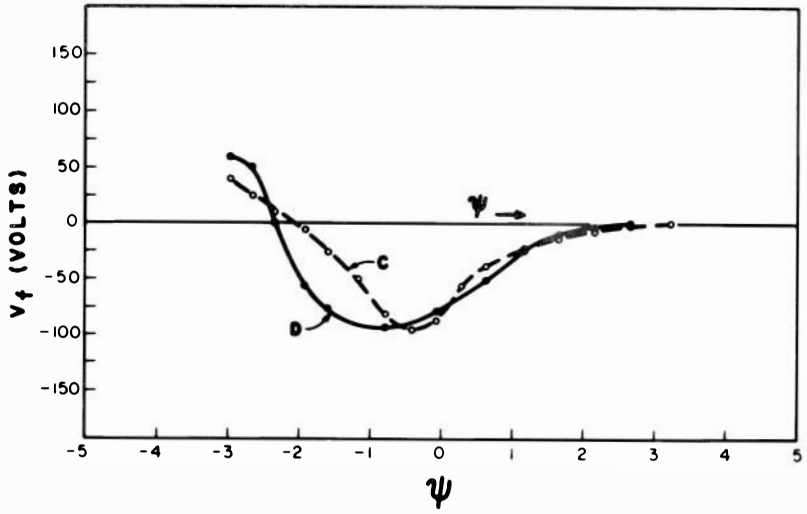

(c)

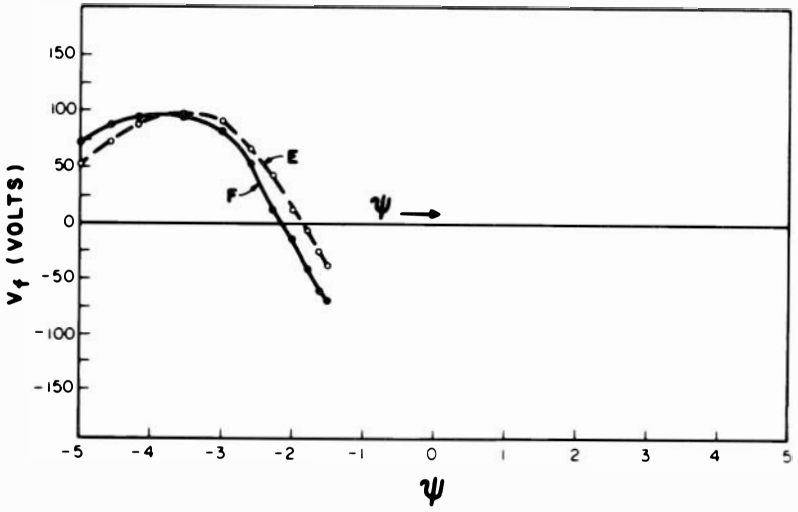

(d)

POTENTIALS AT 15μ SEC. VS. ψ FOR VARIOUS SCANS AT P-8

Fig. 5

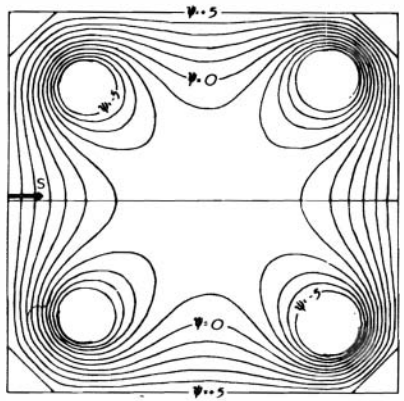

OCTUPOLE FIELD PATTERN

(a)

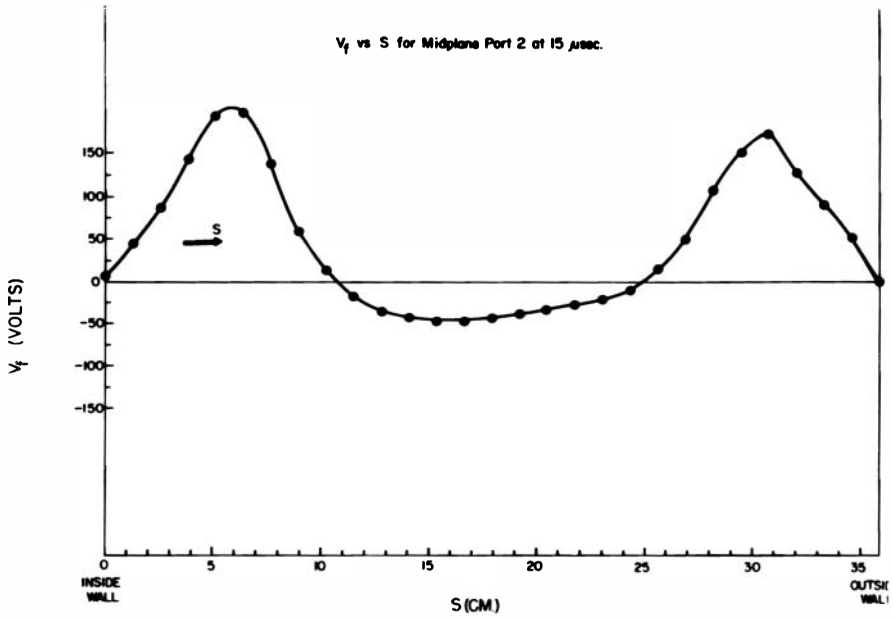

(b)

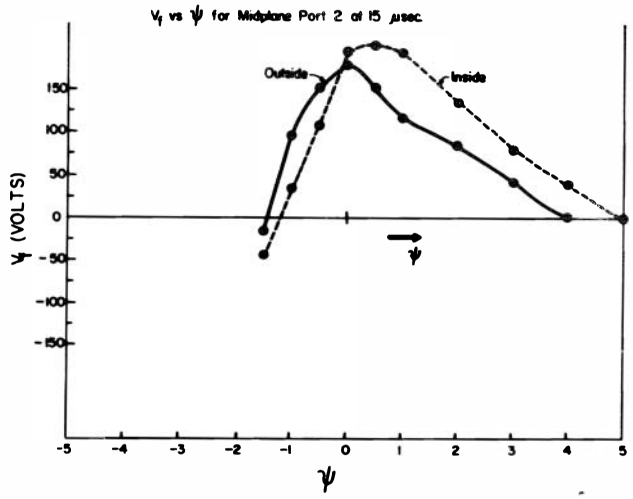

(c)

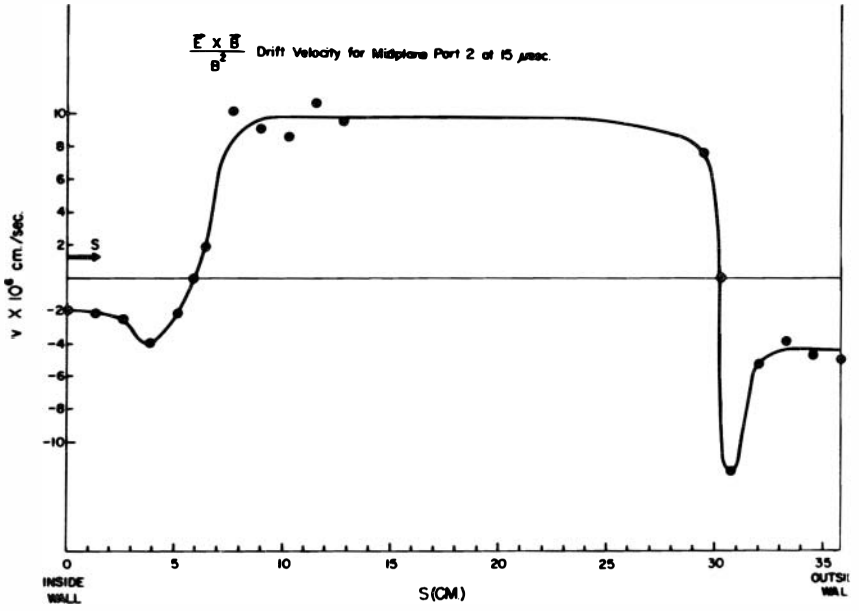

(d)

Fig. 6

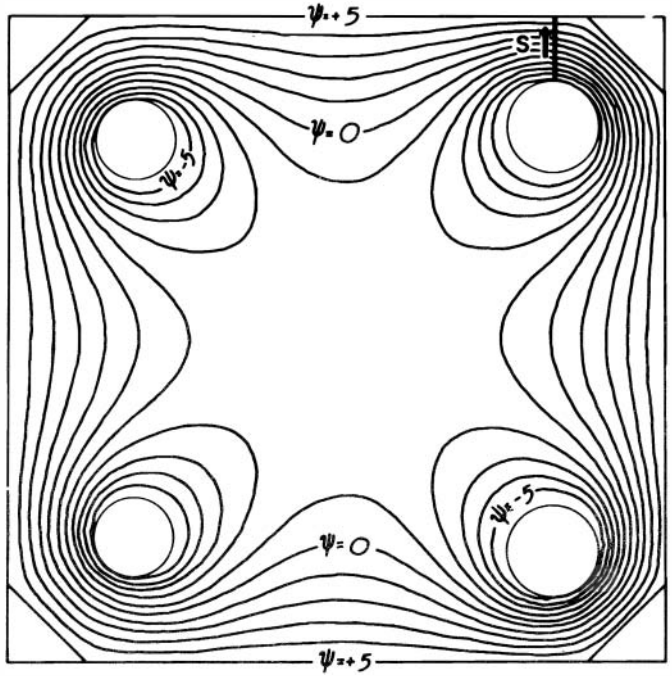

OCTUPOLE FIELD PATTERN

(a)

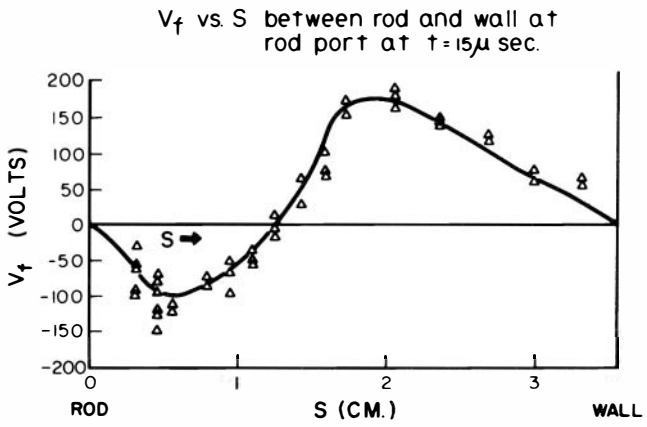

(b)

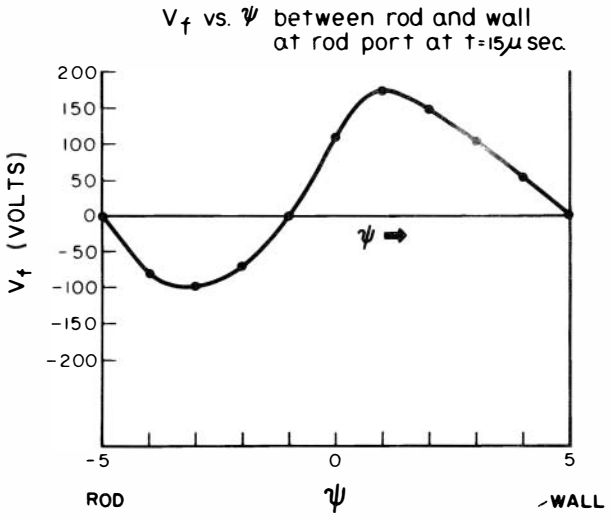

(c)

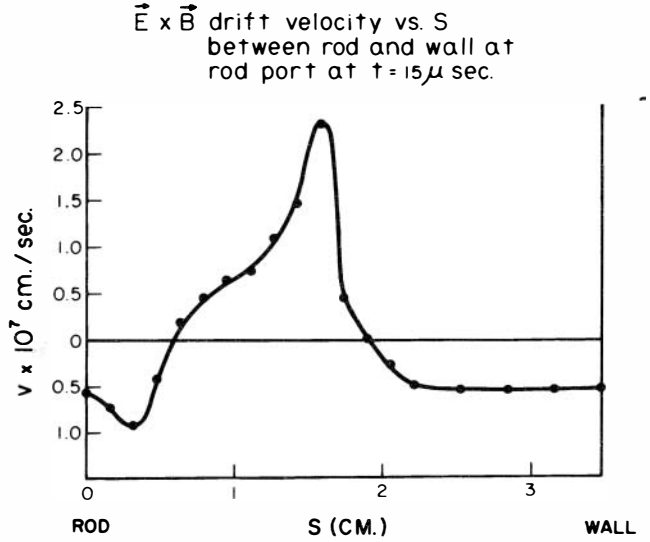

(d)

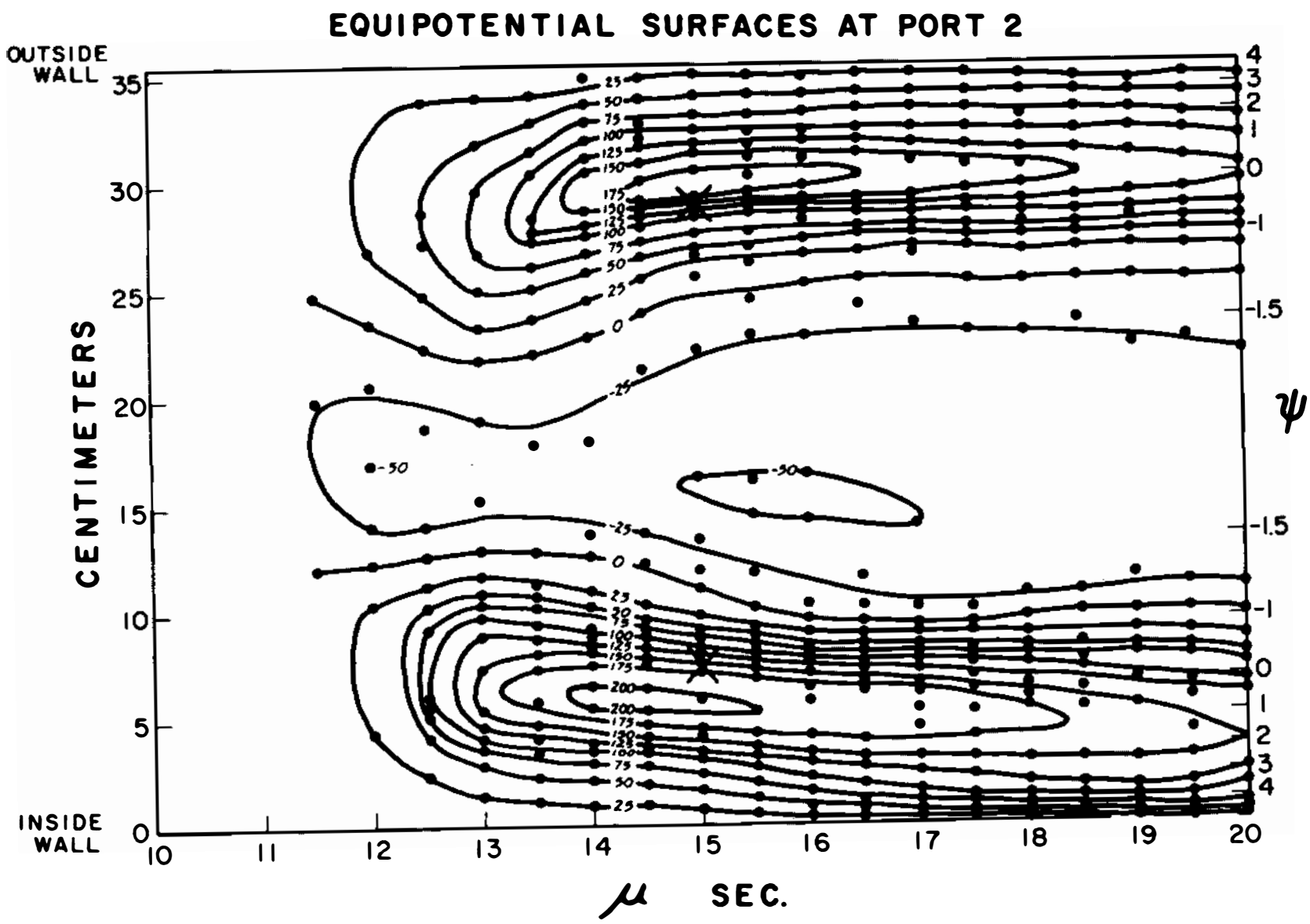
EQUIPOTENTIAL SURFACES AT PORT 2
OUTSIDE WALL
INSIDE WALL
CENTIMETERS
35
30
25
20
15
10
5
0
10
11
12
13
14
15
16
17
18
19
20
μ SEC.
ψ
4
3
2
1
0
-1
-1.5
-1.5
-1
0
1
2
3
4
25
50
75
100
125
150
175
200
-25
-50

Fig. 8

EQUIPOTENTIAL SURFACES AT ROD PORT

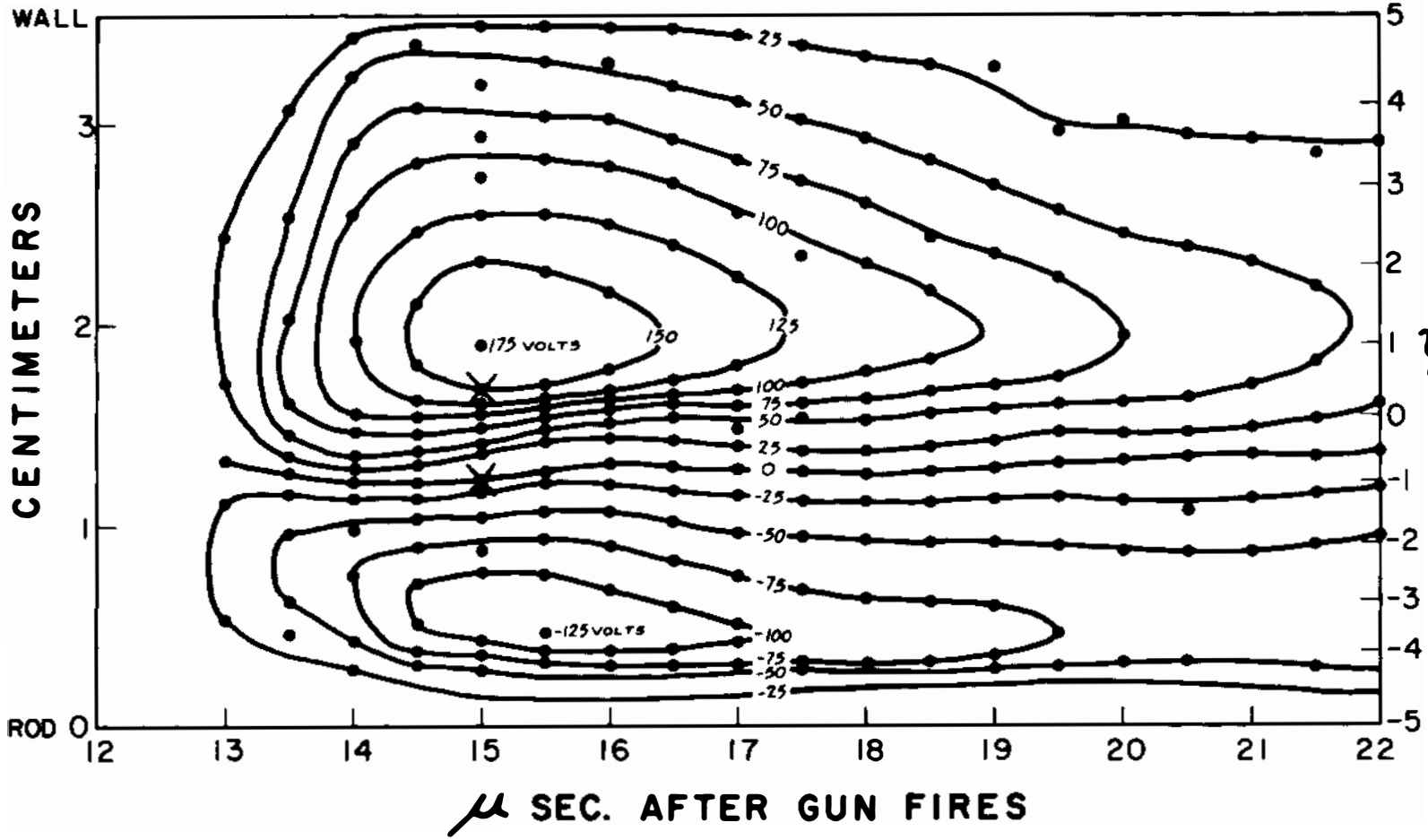

Fig. 9

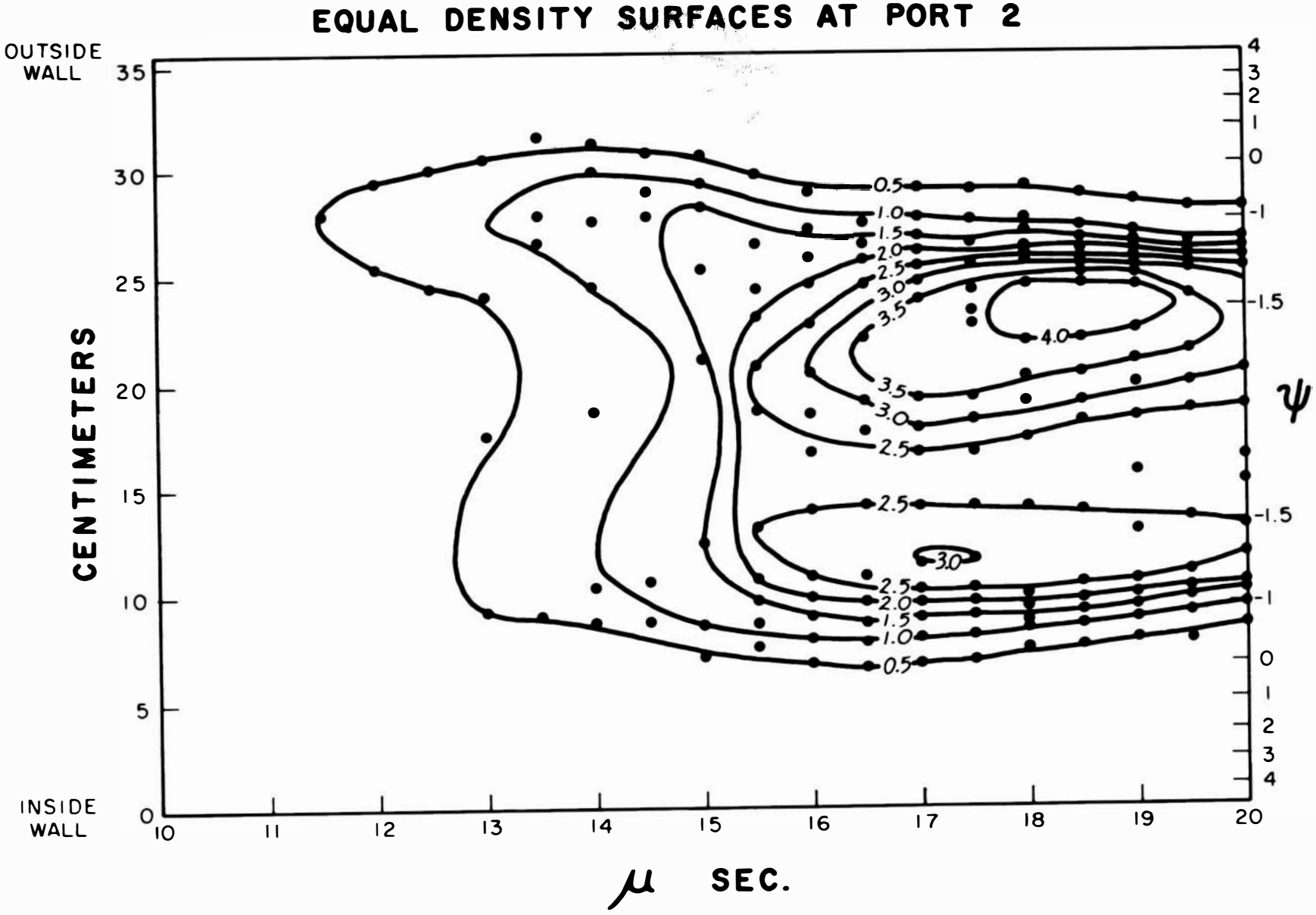
EQUAL DENSITY SURFACES AT PORT 2
OUTSIDE WALL
INSIDE WALL
CENTIMETERS
35
30
25
20
15
10
5
0
10
11
12
13
14
15
16
17
18
19
20
μ SEC.
ψ
4
3
2
1
0
-1
-1.5
-1.5
-1
0
1
2
3
4
0.5
1.0
1.5
2.0
2.5
3.0
3.5
4.0
3.5
3.0
2.5
2.5
3.0
2.5
2.0
1.5
1.0
0.5

Fig. 10